

IntersectGAN: Learning Domain Intersection for Generating Images with Multiple Attributes

Zehui Yao¹, Boyan Zhang¹, Zhiyong Wang¹, Wanli Ouyang^{2,3}, Dong Xu², Dagan Feng¹

¹School of Computer Science, The University of Sydney, Australia

²School of Electrical and Information Engineering, The University of Sydney, Australia

³The University of Sydney, SenseTime Computer Vision Research Group, Australia

{zyao3112,bzha8220}@uni.sydney.edu.au,{zhiyong.wang,wanli.ouyang,dong.xu,dagan.feng}@sydney.edu.au

ABSTRACT

Generative adversarial networks (GANs) have demonstrated great success in generating various visual content. However, images generated by existing GANs are often of attributes (e.g., smiling expression) learned from one image domain. As a result, generating images of multiple attributes requires many real samples possessing multiple attributes which are very resource expensive to be collected. In this paper, we propose a novel GAN, namely IntersectGAN, to learn multiple attributes from different image domains through an intersecting architecture. For example, given two image domains X_1 and X_2 with certain attributes, the intersection $X_1 \cap X_2$ denotes a new domain where images possess the attributes from both X_1 and X_2 domains. The proposed IntersectGAN consists of two discriminators D_1 and D_2 to distinguish between generated and real samples of different domains, and three generators where the intersection generator is trained against both discriminators. And an overall adversarial loss function is defined over three generators. As a result, our proposed IntersectGAN can be trained on multiple domains of which each presents one specific attribute, and eventually eliminates the need of real sample images simultaneously possessing multiple attributes. By using the CelebFaces Attributes dataset, our proposed IntersectGAN is able to produce high quality face images possessing multiple attributes (e.g., a face with black hair and a smiling expression). Both qualitative and quantitative evaluations are conducted to compare our proposed IntersectGAN with other baseline methods. Besides, several different applications of IntersectGAN have been explored with promising results.

CCS CONCEPTS

• **Computing methodologies** → **Computer vision tasks; Learning paradigms.**

KEYWORDS

Image generation, Deep learning, Generative adversarial networks

ACM Reference Format:

Zehui Yao, Boyan Zhang, Zhiyong Wang, Wanli Ouyang, Dong Xu, Dagan Feng. 2019. IntersectGAN: Learning Domain Intersection for Generating Images with Multiple Attributes. In *Proceedings of the 27th ACM International Conference on Multimedia (MM '19)*, October 21–25, 2019, Nice, France. ACM, New York, NY, USA, 9 pages. <https://doi.org/10.1145/3343031.3350908>

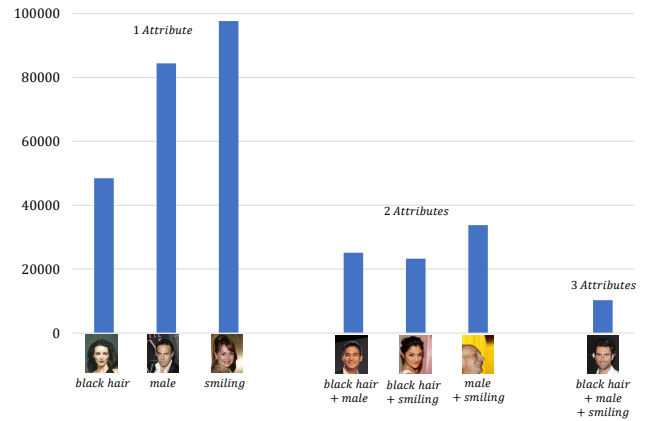


Figure 1: Statistics of the images with single attribute and multiple attributes in the CelebFaces Attributes dataset. The sample attributes and images are for illustration purpose.

1 INTRODUCTION

In recent years, generative adversarial networks (GANs) have achieved promising progress on image generation due to its adversarial training strategy. A GAN model generally consists of two key components, a generator and a discriminator. The generator outputs generated samples (i.e., fake samples) that are as indistinguishable as possible from real samples, while the discriminator differentiates real samples from fake samples (i.e., generated samples) as much as possible. As a result, the generator is able to match the distribution of real samples.

Motivated by the success of generating synthetic data (e.g., digits [4]) for training a better classifier, various GANs-based frameworks have been proposed for different applications such as image style transfer [8, 29, 32], image super resolution [13], high resolution image generation [9, 27], text-based image generation [28, 31], faces image synthesis [2, 19, 26] and fashion designs [20, 34].

When generating images with multiple attributes using conventional GANs, we often need to collect real samples possessing all

Permission to make digital or hard copies of all or part of this work for personal or classroom use is granted without fee provided that copies are not made or distributed for profit or commercial advantage and that copies bear this notice and the full citation on the first page. Copyrights for components of this work owned by others than ACM must be honored. Abstracting with credit is permitted. To copy otherwise, or republish, to post on servers or to redistribute to lists, requires prior specific permission and/or a fee. Request permissions from permissions.acm.org.

MM '19, October 21–25, 2019, Nice, France

© 2019 Association for Computing Machinery.

ACM ISBN 978-1-4503-6889-6/19/10...\$15.00

<https://doi.org/10.1145/3343031.3350908>

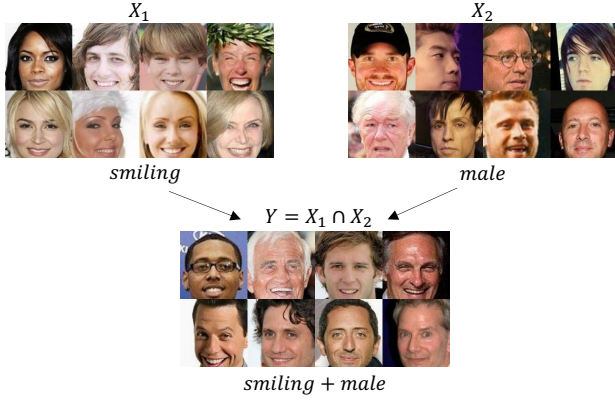


Figure 2: Illustration of intersecting two image domains X_1 and X_2 into a new domain $X_1 \cap X_2$. Domain X_1 contains face samples with attribute *smiling*, domain X_2 contains face samples with attribute *male*, and domain $X_1 \cap X_2$ represents face images with both *smiling* and *male*.

the required attributes and train the networks with the collected images or apply an extension of GAN to a conditional setting. However, as shown in Figure 1, when the number of specified attributes increases, in general, the number of samples decrease dramatically. It is challenging to collect a large number of real samples possessing multiple attributes for training deep networks, and also resource expensive to produce supervision labels. It is anticipated that it will be increasingly challenging when the number of attributes increases.

To overcome such limitation of the existing GANs, we propose a novel GAN model, namely IntersectGAN, to generate images with multiple attributes by learning the distribution of a new domain intersected from existing domains. For simplicity of explanation, we use two domains in the following discussions. Given two image domains X_1 and X_2 with corresponding attributes A_1 and A_2 , respectively. The intersection $Y = X_1 \cap X_2$ denotes a new domain where images possess the attributes from both X_1 and X_2 domains, and the new intersected attribute is denoted as A_Y . That is, the intersected domain $X_1 \cap X_2$ possesses a new attribute A_Y denoted as $A_1 \cup A_2$, which is the combination of both attributes A_1 and A_2 . As illustrated in Figure 2, A_1 is *smiling* and A_2 is *male*. The images in the intersected domain $X_1 \cap X_2$ possess these two attributes simultaneously. That is, $A_{X_1 \cap X_2} = A_1 \cup A_2 = \{\text{smiling, male}\}$.

As illustrated in Figure 3, when generating images with n specified attributes, our proposed IntersectGAN model consists of $n + 1$ generators (i.e., one generator for each attribute and one generator for combined attributes) and n discriminators (i.e., one for each attribute). In comparison with conventional GANs, the discriminators are further challenged to be more discriminant by also taking the input from the intersection generator G_Y . During the training phase, the intersection generator aims to produce content which is as indistinguishable as possible to all n image domains. We define the overall adversarial loss as the summation of the losses from $n + 1$ generators. That is, the intersection generator G_Y is trained to fit the distribution of samples possessing the attributes from

all the given domains. As a result, our proposed IntersectGAN is able to produce synthesized samples possessing multiple attributes without relying on real samples simultaneously possessing those attributes.

Furthermore, we explore the capacity of our proposed IntersectGAN in several other image generation tasks, such as generating images of a blended attribute by intersecting two opposite attributes (e.g., *male* and *female*) and content-aware domain intersection. In addition, by exploiting the interaction among three generators with inter-layer weight sharing, we are able to adapt the IntersectGAN to generate trio image samples, which better illustrates the idea of learning domain intersection.

In summary, the key contributions of our work are as follows:

- (1) We propose a novel IntersectGAN model which is able to generate image samples possessing multiple attributes without using real samples simultaneously possessing those attributes. To the best of our knowledge, this is the first GAN model specially developed for generating images with multiple attributes from noise input by learning a domain intersection without introducing supervision labels.
- (2) We formulate the intersection learning problem under the GAN framework to learn the distribution of an intersection of multiple domains. New adversarial training strategies are proposed to take into account the new architecture: the discriminators are trained against the parallel generators of individual domains plus the intersection generator while the intersection generation is trained against all the discriminators.
- (3) We demonstrate the capacity of the proposed IntersectGAN in other image generation applications, such as generating images with a blended attribute and generating content-aware domain intersected images. In particular, a weight sharing architecture (as illustrated in dashed lines in Figure 3) is proposed to explore the relationship among generators and generate trio images. More details of weight sharing are explained in Section 5.3.

2 RELATED WORK

In this section, we organize GAN based image generation methods into two categories: image generation and image-to-image translation, in terms of whether a real input image is needed for the generator. The first category aims to generate image samples from a noise vector after learning the distribution of an image domain, while the second category aims to generate a new version of each given image by translating the input sample to another image domain.

2.1 Image Generation

GAN [4] was first proposed to learn a target distribution with an adversarial learning strategy, and has dramatically accelerated the progress on image generation. It has been widely utilized to generate image samples of the same style as of the given training image set. Various other improvements for GANs have been developed, such as network architectures, loss functions, and optimization strategies. For example, DCGAN [25] was proposed to boost the

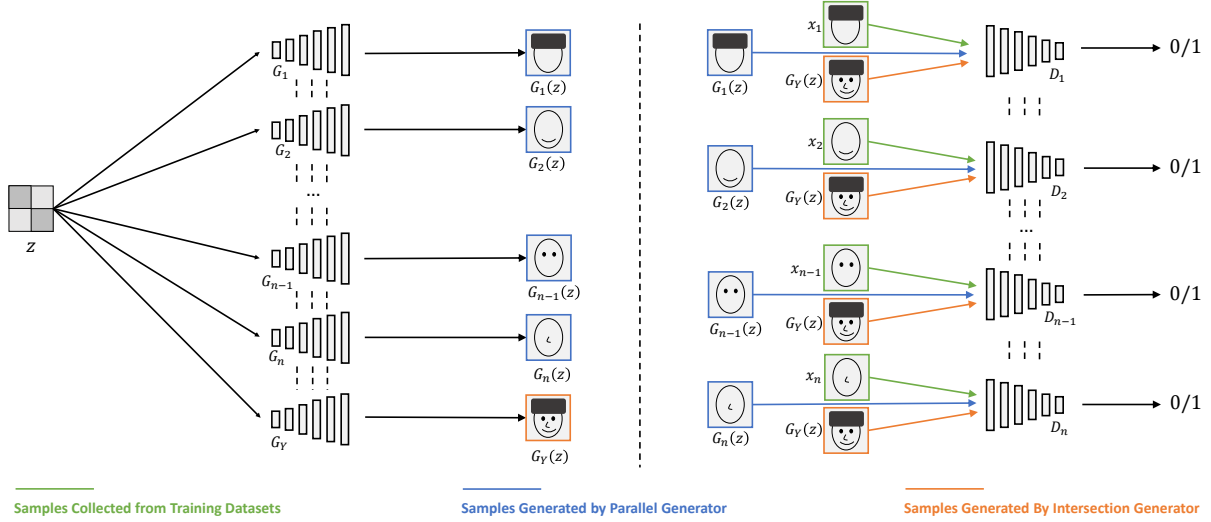


Figure 3: Illustration of our proposed IntersectGAN model which consists of n parallel generators $G_1, G_2, \dots, G_{n-1}, G_n$ and an intersection generator G_Y as well as n discriminators D_1, D_2, \dots, D_{n-1} and D_n . Note that z denotes the random noise input, x_1, x_2, \dots, x_{n-1} and x_n are the real samples collected from the corresponding image domains X_1, X_2, \dots, X_{n-1} and X_n , respectively. The generators produce fake image samples $G_1(z), G_2(z), \dots, G_{n-1}(z), G_n(z)$ and $G_Y(z)$, while the discriminators would output a value ranging from 0 to 1 indicating the probability whether an input image is a real sample. The dash lines between generators (discriminators) represent optional modifications on the network architecture (e.g., weight sharing).

generative performance of GAN with a new architecture consisting of convolution layers instead of using max pooling or fully connected layers. Many GANs have also been proposed by using new forms of cost functions (e.g., L2 loss and L1 loss etc.) to boost the training process, such as LSGAN [21], WGAN [1], WGAN-GP [5]. However, these GANs take only one image set (i.e., image domain) and follow the one-to-one adversarial learning strategy, namely, one generator is trained against one discriminator. When generating images of multiple attributes through these GANs, real samples simultaneously possessing those attributes are required. However, building qualified dataset is expensive and sometimes even impractical.

In order to influence the content of a generated image in addition to the style, conditional GAN (cGAN) [22] was proposed by adding content labels as an additional input to both generator and discriminator. As a result, the content of generated images is supposed to be of the same as of the specified label, and the style of generated images will be of the same as of the given training images. However, as a supervised learning approach, even for its state-of-the-art cGAN with Projection Discriminator [23], cGAN requires a large number of samples with supervision labels, which are expensive to obtain. Our proposed IntersectGAN is able to address this limitation through its intersection architecture. That is, only the samples possessing individual attributes are required to train IntersectGAN for generating images with multiple attributes and no supervision labels are systematically needed.

2.2 Image-to-Image Translation

Image-to-image translation is a vision and graphics problem aiming to learn a mapping between an input image domain and a target image domain with two training datasets (one dataset for each domain). Pix2pix [8] was first proposed to perform one-way image-to-image translation through a supervised learning approach. A pair of samples (e.g., a sketch image and a color image) is required for both the generator and discriminator. In order to loose the requirement on paired training samples, various GANs have been proposed, such as UNIT [15] and CycleGAN [33], DiscoGAN [10], DualGAN [30]. However, these GANs are limited to translate a given image of one domain to an image of the other domain.

Three recently proposed GANs, IcGAN [24], conditional CycleGAN [18] and StarGAN [2], are able to translate a given image into an image with multiple attributes through conditional input labels. However, label information is required during the training as the conditional configuration. Differently, our IntersectGAN is proposed for image generation from noise input, instead of image-to-image translation, and supervision label information is not required during training.

3 INTERSECTGAN

In this section, we first present the formulation of IntersectGAN and then explain its implementation details.

3.1 Formulation

Given image domains $X_1, X_2 \dots X_n$ specified with n attributes $A_1, A_2 \dots A_n$, respectively, IntersectGAN aims to learn a mapping from random noise to the target domain $Y = \bigcap_{1 \leq i \leq n} X_i$ where generated

samples are supposed to possess all the specified attributes. We denote the distribution of real image samples as $x_i \sim p_{X_i}$ for $1 \leq i \leq n$. In addition, the distribution of random noise is denoted as $z \sim p_Z$. During the training phase, our model learns n parallel mappings $G_i : Z \rightarrow X_i$ and an intersection mapping $G_{\text{Intersect}} : Z \rightarrow Y$. Meanwhile, there are n discriminators $D_1, D_2 \dots D_n$ distinguishing between real and generated samples with regard to the corresponding domains $X_1, X_2 \dots X_n$, respectively. In the training stage, the expected output of a discriminator for a real image is set to 1, and that for a generated image is set to 0.

Motivated by GAN, our proposed IntersectGAN is formulated through the definition of adversarial loss. According to the objective of GAN, for an image domain X , a generator G and a corresponding discriminator D , the adversarial loss function is defined as:

$$\mathcal{L}_{\text{GAN}}(X, G, D) = \mathbb{E}_{x \sim p_X} [\log D(x)] + \mathbb{E}_{z \sim p_Z} [\log (1 - D(G(z)))], \quad (1)$$

where G is trained to generate synthetic images $G(z)$ possessing the attribute of domain X while D tries to differentiate real image samples x from generated samples $G(z)$.

As illustrated in Figure 3, IntersectGAN has n parallel generators $G_1, G_2, \dots G_n$ as well as n corresponding discriminators D_1, D_2, \dots, D_n . Their adversarial losses can be expressed as:

$$\mathcal{L}_i = \alpha_i \mathcal{L}_{\text{GAN}}(X_i, G_i, D_i), \text{ for } 1 \leq i \leq n, \quad (2)$$

where α_i indicates the objective importance of the i -th parallel generator.

The intersection generator G_Y produces image samples containing all the specified attributes $A_1, A_2 \dots A_n$. Ideally, each discriminator D_i cannot distinguish between the generated samples $G_Y(z)$ and real images from its corresponding domain X_i . Therefore, we can formulate the objective of G_Y as a weighted sum of n adversarial losses:

$$\mathcal{L}_{\text{Intersect}} = \sum_{1 \leq i \leq n} \alpha_i \mathcal{L}_{\text{GAN}}(X_i, G_Y, D_i), \quad (3)$$

where α_i is the importance constant mentioned above and G_Y aims to simultaneously minimize two adversarial losses against both discriminators.

For the whole model, the overall adversarial loss is:

$$\mathcal{L}_{\text{IntersectGAN}} = \sum_{1 \leq i \leq n} \mathcal{L}_i + \lambda_{\text{Intersect}} \mathcal{L}_{\text{Intersect}}, \quad (4)$$

where $\lambda_{\text{Intersect}}$ is a constant controlling the relative significance among different objectives. During the training phase, the optimization problem can be formulated as a minimax game where the generative model tries to minimize the objective while discriminators aim to maximize it, and the goal is to find appropriate parameters for the intersection generator. This is given by:

$$G_Y^* = \arg \min_{G_i, G_Y} \max_{D_i} \mathcal{L}_{\text{IntersectGAN}}, \text{ where } 1 \leq i \leq n. \quad (5)$$

The optimization aims to find an appropriate set parameters where the intersection generator can produce most realistic samples.

The core idea of the proposed IntersectGAN model is reflected in two parts:

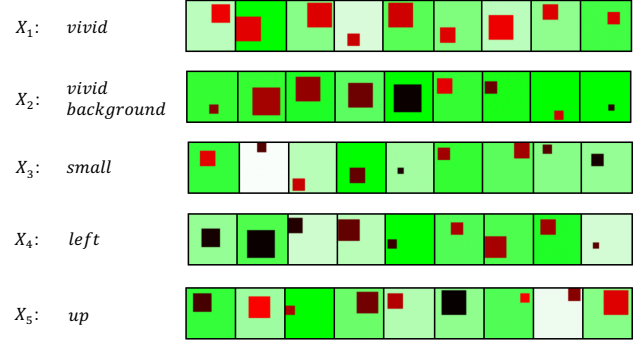


Figure 4: Image samples from Colored Square dataset used in the experiments. Domains X_1, X_2, X_3, X_4 and X_5 are specified with attributes *vivid*, *vivid background*, *small*, *left* and *up* respectively.

- (1) The existence of parallel generators G_i is for boosting their adversaries D_i to better distinguish real samples and fake samples;
- (2) All the discriminators D_i are the adversaries of G_Y , which allows the intersection generator to learn all the attributes presented in those given domains.

3.2 Implementation

Revised Adversarial Loss Function In order to stabilize the training outcomes and help models to converge better, we follow the strategy used in Wasserstein GAN [1] to define a new objective function by introducing the gradient penalty [5]. Then the loss function defined in Equation (1) can be re-formulated as:

$$\mathcal{L}_{\text{GAN}}(X, G, D) = \mathbb{E}_{x \sim p_X} [D(x)] - \mathbb{E}_{z \sim p_Z} [D(G(z))] - \lambda_{pg} \mathbb{E}_{\hat{x} \sim p_{\hat{x}}} [(\|\nabla_{\hat{x}} D(\hat{x})\|_2 - 1)^2], \quad (6)$$

where \hat{x} is uniformly sampled from the linear space between a pair of real and generated images.

Architecture Deep convolutional neural networks [25] are used to implement IntersectGAN, which is constructed with $n + 1$ structurally identical generator networks and n discriminator networks. When generating sample images with the size of 128×128 , we fix the dimension of input noise to 32. All the generators consist of one fully connected layer and seven deconvolutional layers. All the discriminators contain six convolutional layers and two fully connected layers to output a single logit indicating the probability whether the input sample is real. Batch normalization [7] and layer normalization [14] are utilized for generators and discriminators, respectively. Note that the relationship among generators (discriminators) can be explored through weight sharing as explained in Section 5.3.

Training During the training phase, we apply random cropping and flipping to real input images in order to enhance sample variety. All the input vectors of random noise are sampled from the standard normal distribution. The batch size of input data is 32. We use Adam optimizer [11] to train the model with $\beta_1 = 0.5$ and $\beta_2 = 0.999$. In addition, the initial learning rate was set to 0.0002. We train the model for 20,000 iterations and apply linear decay on the learning

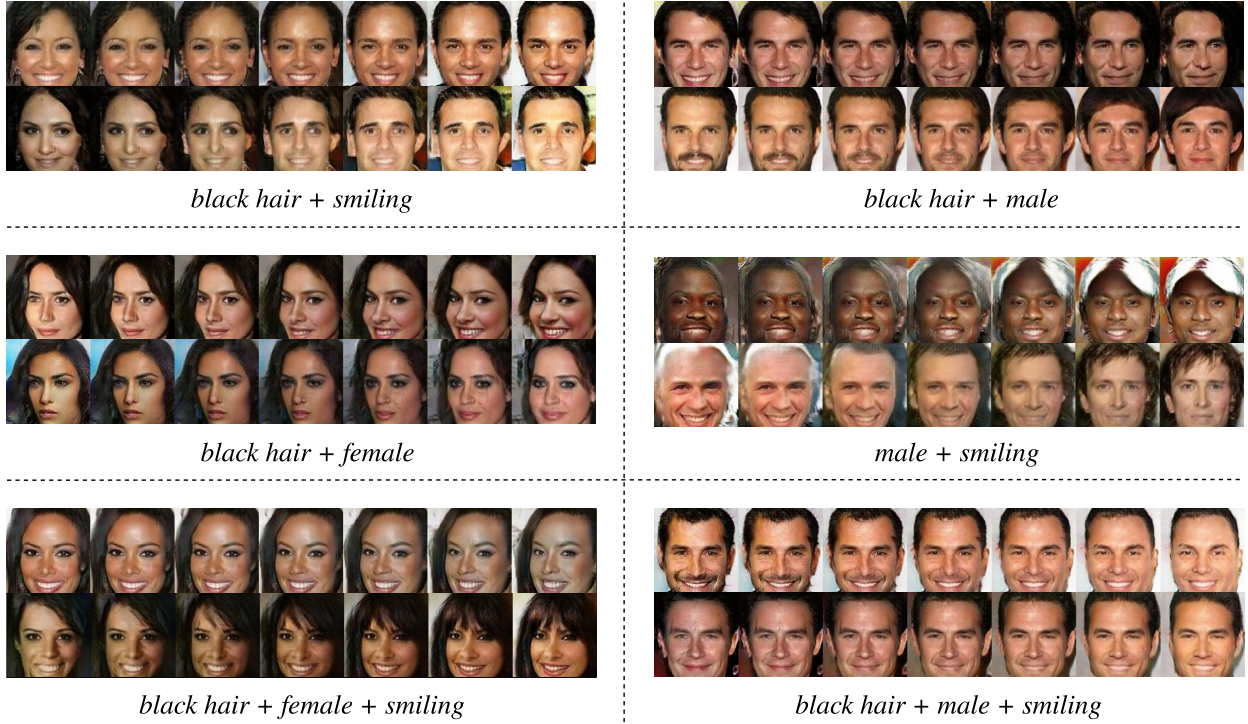


Figure 5: Sample face images with two or three attributes that are generated by our proposed IntersectGAN.

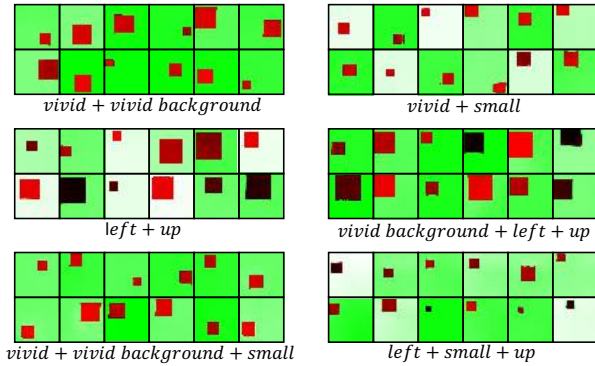


Figure 6: Generated samples of images in different experiments with the Colored Squares dataset.

rate in the second 10,000 iterations to stabilize the training phase. We assume all the attributes are equally important (i.e. $\alpha_i = 1.0$ for all $1 \leq i \leq n$) and set $\lambda_{\text{Intersect}}$ and λ_{gp} to 1.0 and 10.0 respectively in all the experiments.

4 EXPERIMENTAL RESULTS AND DISCUSSIONS

In this section, we first present two experiments for qualitative evaluation: a preliminary experiment on generating colored squares, and a comprehensive experiment on generating face images with

multiple attributes. Then a set of experiments are introduced for quantitative evaluation against several baseline algorithms.

4.1 Experiments

Generating Multi-Attribute Squares In the experiment, as illustrated in Figure 4, 5 specific visual attributes are utilized to describe the colored square images: *vivid* (i.e. the color of a square is closer to pure red), *vivid background* (i.e. the background color is closer to pure green), *small*, *left* and *up*. An image dataset of Colored Squares was purpose-built for validating the objective of IntersectGAN. It consists of 5 groups of images and each of them contain 2000 image samples of a colored square. Each group corresponds to one visual attribute and all the images in that group contain the a specific attribute and other attributes are randomly generated. All the samples are generated randomly by our computer program and all the random factors (e.g. color) are sampled from uniform distributions. It is likely that there is no exact same image that appears in two image groups. In the experiment, the goal is to generate images possessing all the specific attributes after training our proposed IntersectGAN with the given training datasets. Sample results of each experiment can be found in Figure 6, which indicates that IntersectGAN is able to generate image samples with multiple specific attributes.

Generating Multi-Attribute Faces We use CelebFaces Attributes (CelebA) Dataset [17] to train baseline models for generating faces images with multiple attributes. There are 202,599 annotated image samples of celebrity faces in the dataset. According to the annotations, before training the model, we partition the dataset into

different domains in terms of specified visual attributes. As shown in Figure 5, our proposed IntersectGAN is able to produce high quality two-attribute and three-attribute face images. In each row, the samples generated are gradually changed from one face to the other by linearly changing the input noise vector. For example, each of the two-attribute samples *black hair + smiling* clearly present such two attributes, although the *gender* attribute does not affect the results.

4.2 Metrics

Fréchet Inception Distance (FID) [6] As a quantitative measurement of GAN proposed recently, *FID score* is used to estimate the generating quality of baseline models by measuring the Fréchet distance between generated samples and real samples. For each face generation experiment with certain combination of specified attributes, we collect ground truths from CelebA datasets according to the given annotations and face image samples generated by each baseline model that is supposed to simultaneously contain all the specified attributes.

Perceptual Study As evaluating image realism and identifying facial attributes can be subjective, we conduct two perceptual studies with Amazon Mechanical Turk (AMT) system. To estimate the realism of the samples generated by each model, we obtain a *Realism Score* for each model by using AMT to perform human based perceptual survey. At first, 1000 groups of image samples were generated from different models (i.e., our proposed IntersectGAN and the baseline models) and each group contains one image sample generated by each model with the same noise input. In the survey, a Tucker was shown a number of image groups and asked to select the most realistic one from each group. To ensure the quality of data collection from Turkers, we set additional qualifications to only allow workers whose Approval Rate is greater than 95% to participate in the survey and also assign a few questions with apparent answers to validate their effort. After all the image groups are examined, we obtain the Realism Score for each model by calculating the percentage of sample images generated by the model that Tuckers selected as the most realistic ones.

To further examine the presence or absence of specified attributes in the generated samples, we design another human based perceptual survey using AMT to obtain *Attribute Score* for each model. In the survey, a Turker was shown a number of generated image samples and for each given sample the Turker was asked to answer three multiple choice questions in regard to specific attributes including hair color, expression, and gender. For example, for gender attribute, the given choices are *Male*, *Female* and *Cannot identify*. In order to reduce the bias caused by random selection, in the experiment, 300 image samples were generated by each model for examination. After all the tasks are finished, we derive the Attribute Score for each model by calculating the percentage of image samples generated by the model that simultaneously possesses all the specified attributes.

4.3 Baselines

Conditional GAN with Projection Discriminator (cGAN PD) As one of the-state-of-art GAN-based architectures with additional supervision inputs, conditional GAN with projection discriminator

Methods	B+M	M+S	F+S	B+M+S	B+F+S
cGAN PD	84.6	93.8	69.9	94.2	73.5
D2GAN*	90.0	96.9	64.9	97.0	81.6
IntersectGAN	77.9	79.9	64.5	83.5	72.3

Table 1: Comparison results in terms of FID for different attribute combinations of the experiments with CelebA datasets where B, F, M and S denote the attributes *black hair*, *female*, *male* and *smiling*, respectively.

[23] is used as one of the baseline model. n labels (i.e., 0/1) are given to indicate whether an output image should respectively contain each attribute. As a supervised learning method, in its implementation, the label of each image needs to be available, which means that it has stronger or stricter requirements than ours.

GAN with Dual Discriminators (D2GAN*) This model has the identical structure with the D2GAN model proposed by Nguyen et al. [3]. Two discriminators in the original D2GAN learn from the same datasets. However, in the comparison experiments, they were trained from different image domains. When the number of specified attributes is more than 2, we increase the number of discriminators correspondingly. The comparison with this model can help tell how much the quality of generated image samples would increase when a model contains multiple parallel generators. For the sake of convenience, we denote the modified model as D2GAN* in this paper.

4.4 Comparisons

In each comparison experiment, we specify n attributes and collect real samples of these attributes to build the training datasets X_i for $1 \leq i \leq n$. The CelebA dataset is used in all the following comparison experiments. For fair comparison, we use an identical architecture to implement all the models and train them under the same configuration.

For qualitative comparison, as shown in Figure 7, the image samples generated by our proposed IntersectGAN are generally of highest visual quality, while those by other baselines are of lower visual quality (e.g., artifacts and unnatural skin color). In addition, the image samples generated by our IntersectGAN present clear attributes than those generated by other GANs, as IntersectGAN aims to *fool* all the discriminators corresponding to each attribute.

For quantitative comparison, we conduct experiments with 5 combined attributes, including *black hair + male*, *male + smiling*, *female + smiling*, *black hair + male + smiling*, and *black hair + female + smiling*. As illustrated in Table 1, our proposed IntersectGAN achieves lowest FID scores in all the comparative experiments. D2GAN* is inferior in all the comparisons as well, which indicates the boosting effect of parallel generators. Without any supervision labels, our proposed IntersectGAN performs even better than cGAN PD for the lower FID scores. The comparison results indicate that our proposed IntersectGAN performs better for generating samples of higher quality and diversity than other baseline models.

For perceptual studies, as shown in Table 2, IntersectGAN achieves significantly higher Realism Score than other baselines models,

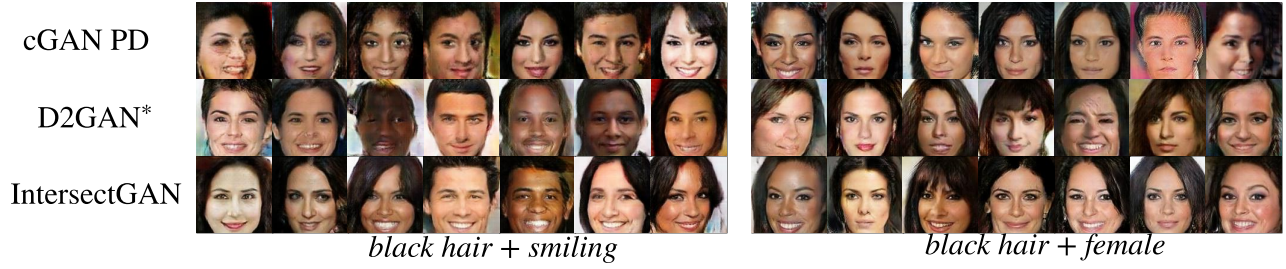


Figure 7: Sample multi-attribute face images generated by different GAN models trained on the CelebA images. The example on the left represents the combined attributes *blackhair* and *smiling* and the example on the right represents the combined attributes *blackhair* and *female*.

Methods	<i>B+M</i>	<i>M+S</i>	<i>F+S</i>	<i>B+M+S</i>	<i>B+F+S</i>
cGAN PD	31.7%	40.0%	22.6%	27.8%	21.8%
D2GAN*	16.2%	16.5%	23.9%	25.5%	32.5%
IntersectGAN	52.1%	43.5%	53.5%	46.7%	45.7%

Table 2: Comparison results in terms of Realism Score for different attribute combinations.

Methods	<i>B+M</i>	<i>M+S</i>	<i>F+S</i>	<i>B+M+S</i>	<i>B+F+S</i>
cGAN PD	80.6%	69.0%	83.0%	41.6%	46.6%
D2GAN*	52.6%	41%	68.6%	23.6%	20.6%
IntersectGAN	87.0%	81.3%	91.3%	47.6%	53.6%
Ground Truths	12.4%	16.7%	31.5%	5.1%	6.4%

Table 3: Comparison results in terms of Attribute Score for different attribute combinations.

which means that our IntersectGAN is able to generate more realistic image samples than other baseline models. It is expected that the advantage will be more obvious when the number of attributes increases.

As shown in Table 3, our IntersectGAN also achieves considerably high Attribute Scores in the experiments. Percentages of image samples possess all the specified attributes are given as a reference. Our proposed IntersectGAN achieves highest Attribute Scores in all the comparisons which are much higher than the ground truth percentage. It demonstrates the advantage of our model that it is able to synthesize high quality images of multiple attributes without relying on real image samples possessing those attributes. As for cGAN PD and D2GAN*, in addition to the potentially poorer capability to enforce output images to contain both specified attributes, the low realism of their generating samples can also negatively influence the Attribute Score.

5 OTHER APPLICATIONS

In this section, we explore the generation capacity of IntersectGAN for three interesting applications: generating images of a blended attribute from two opposite attributes, generating content-aware domain intersected images, and generating trio images.

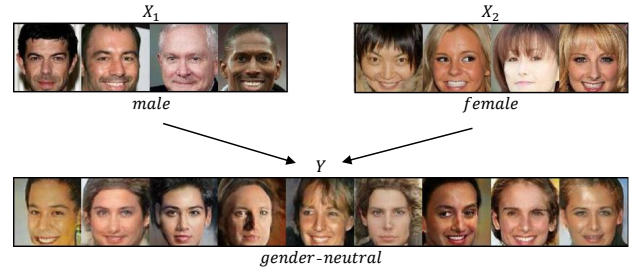


Figure 8: Gender neutral image samples generated by our IntersectGAN from the *male* and *female* face domains.

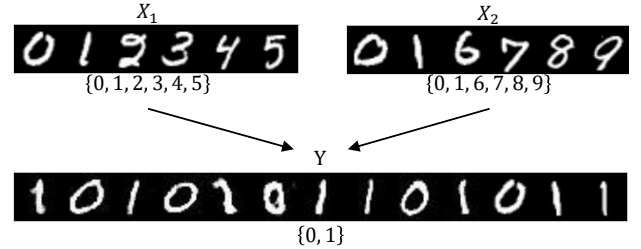


Figure 9: Illustration of content-aware image domain intersection with the MNIST dataset. Domain X_1 contains images of 0, 1, 2, 3, 4, 5 and X_2 consists of 0, 1, 6, 7, 8, 9. The $X_1 \cap X_2$ row displays the generated samples of the intersected domain containing two digits 0 and 1 only.

5.1 Generating Images of Blended Attributes

Semantic attribute indicates the presence or absence of certain characteristics in an image, which can be regarded as a binary value. When these attributes are independent of each other, intersecting such attributes leads to the combination of these attributes. However, when such attributes contradict to each other, such as gender, intersection would lead to a blending effect on such attributes, which is a unique outcome of our IntersectGAN, in comparison with cGAN and its variants.

In the experiment, we divide the CelebA dataset into two sets: *male* image set and *female* image set, according to the annotations

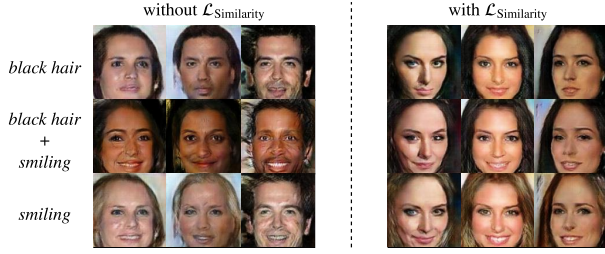


Figure 10: The effect of similarity loss for generating trio image samples. The specified attributes in the comparative experiment are *black hair* and *smiling*.

provided. For IntersectGAN, domain X_1 and domain X_2 possess the attributes *male* and *female*, respectively. According to the intersection nature of IntersectGAN, it is expected that the generated image samples will possess both *male* and *female* attributes.

In other words, generated images of such two attributes would be gender-neutral. As shown in Figure 8, it is not easy to tell the gender of the generated image samples in the bottom row.

5.2 Generating Content-aware Domain Intersected Images

This task is to demonstrate that the proposed IntersectGAN is able to generate images with both content and attribute intersected from two domains. Assume we have two image domains X_1 and X_2 where X_1 contains images of content c_{i_1}, c_{i_2}, \dots , and images in X_2 are of content c_{j_1}, c_{j_2}, \dots . For both image domains, we denote the set of content items as C_1 and C_2 , and the set of intersected content items as $C_1 \cap C_2$.

We train our model on the MNIST dataset [12] for this task. As shown in Figure 9, domain X_1 contains images of digits 0, 1, 2, 3, 4, 5, domain X_2 contains images of digits 0, 1, 6, 7, 8, 9, and the intersected domain Y contains generated samples of 2 digits 0 and 1 only which is the intersection of two sets $\{0, 1, 2, 3, 4, 5\}$ and $\{0, 1, 6, 7, 8, 9\}$.

5.3 Generating Trio Images

To better visualize the objective of multi-attribute image generation by learning domain intersection, we change the network architecture of IntersectGAN to generate image samples in trio which are visually similar. We follow the idea from CoGAN [16] and share the weights in the first several layers of three generators in our model. In addition, discriminators D_1 and D_2 share the weights except the first two layers. This architecture allows IntersectGAN to generate samples in pair. Then for each input noise z , we can generate samples in trio denoted as $G_1(z)$, $G_2(z)$ and $G_Y(z)$, respectively, where $G_1(z)$ and $G_2(z)$ are the samples produced by two parallel generators and the sample $G_Y(z)$ would contain the typical attributes of both domain X_1 and X_2 . Ideally, all three generated samples are supposed to look visually similar in some ways.

In addition to the existing objective of IntersectGAN, to improve the correspondence of each trio of output samples, we introduce an



Figure 11: Illustration of trio-image samples. From the top to bottom, image samples are generated by G_1 , G_Y and G_2 . The specified domain attributes are *female* and *black hair*.

additional loss for image generation, namely *similarity loss* denoted as a L1 loss:

$$\mathcal{L}_{\text{Similarity}} = \mathbb{E}_{z \sim p_Z} [\|G_1(z) - G_Y(z)\|_1] + \mathbb{E}_{z \sim p_Z} [\|G_2(z) - G_Y(z)\|_1]. \quad (7)$$

Its objective is to enforce the similarity between $G_Y(z)$ (the output of the intersection generator) and $G_1(z)$ and $G_2(z)$ (the outputs of the two domain generators). A coefficient $\lambda_{\text{Similarity}}$ is introduced to balance the importance of such similarity loss and we set it to 10 in our experiments. Without $\mathcal{L}_{\text{Similarity}}$, although the generated images $G_Y(z)$ contain both specified attributes (e.g., *black hair* and *smiling expression*), they may look far from the corresponding samples generated by the parallel generators on other aspects (e.g., skin color and image background), as shown in Figure 10.

As shown in Figure 11, we generate several groups of trio-image samples with IntersectGAN. We observed that each trio set appears visually similar while the image samples in domain $X_1 \cap X_2$ still contains the attributes intersected from domains X_1 and X_2 .

6 CONCLUSION

In this paper we present a novel IntersectGAN framework to learn intersection of multiple image domains for generating image samples possessing multiple attributes without using real samples simultaneously possessing those attributes. To the best of our knowledge, this is the first GAN model generating multi-attribute images from noise input without introducing extra supervision labels. Both qualitative and quantitative evaluations have demonstrated that our proposed IntersectGAN is able to produce high quality images possessing multiple attributes from separate image sets possessing each individual attribute, rather than from real image samples possessing multiple attributes which are generally expensive to collect. The generation capacity of the proposed IntersectGAN is further explored for three applications: generating images of a blended attribute, content-aware domain intersection based image generation, and trio-image generation. In our future work, we will further extend this model to deal with more attributes with more scalable network architectures.

ACKNOWLEDGEMENTS

This research was partially supported by ARC (Australian Research Council) grant DP160103675. Dong Xu is supported by ARC Future Fellowship FT180100116. We would like to thank the NVIDIA Corporation for GPU support through NVIDIA Hardware Grant.

REFERENCES

- [1] M. Arjovsky, S. Chintala, and L. Bottou. 2017. Wasserstein Generative Adversarial Networks. In *Proceedings of the 34th International Conference on Machine Learning*.
- [2] Y. Choi, M. Choi, M. Kim, J. Ha, S. Kim, and J. Choo. 2018. StarGAN: Unified Generative Adversarial Networks for Multi-Domain Image-to-Image Translation. In *The IEEE Conference on Computer Vision and Pattern Recognition*.
- [3] T. Dinh Nguyen, T. Le, H. Vu, and D. Phung. 2017. Dual Discriminator Generative Adversarial Nets. *ArXiv preprint arXiv: 1709.03831* (2017).
- [4] I. J. Goodfellow, J. Pouget-Abadie, M. Mirza, B. Xu, D. Warde-Farley, S. Ozair, A. Courville, and Y. Bengio. 2014. Generative Adversarial Networks. *ArXiv preprint arXiv: 1406.2661* (2014).
- [5] I. Gulrajani, F. Ahmed, M. Arjovsky, V. Dumoulin, and A. Courville. 2017. Improved Training of Wasserstein GANs. *ArXiv preprint arXiv: 1704.00028* (2017).
- [6] M. Heusel, H. Ramsauer, T. Unterthiner, B. Nessler, and S. Hochreiter. 2017. GANs Trained by a Two Time-Scale Update Rule Converge to a Local Nash Equilibrium. In *Advances in Neural Information Processing Systems 30*.
- [7] S. Ioffe and C. Szegedy. 2015. Batch Normalization: Accelerating Deep Network Training by Reducing Internal Covariate Shift. *ArXiv preprint arXiv: 1502.03167* (2015).
- [8] P. Isola, J. Zhu, T. Zhou, and A. Efros. 2017. Image-To-Image Translation With Conditional Adversarial Networks. In *The IEEE Conference on Computer Vision and Pattern Recognition*.
- [9] T. Karras, T. Aila, S. Laine, and J. Lehtinen. 2017. Progressive Growing of GANs for Improved Quality, Stability, and Variation. *ArXiv preprint arXiv: 1710.10196* (2017).
- [10] T. Kim, M. Cha, H. Kim, J. K. Lee, and J. Kim. 2017. Learning to Discover Cross-Domain Relations with Generative Adversarial Networks. *ArXiv preprint arXiv: 1703.05192* (2017).
- [11] D. P. Kingma and J. Ba. 2014. Adam: A Method for Stochastic Optimization. *ArXiv preprint arXiv: 1412.6980* (2014).
- [12] Y. LeCun and C. Cortes. 2010. MNIST handwritten digit database. <http://yann.lecun.com/exdb/mnist/>. (2010).
- [13] C. Ledig, L. Theis, F. Huszar, J. Caballero, A. Cunningham, A. Acosta, A. Aitken, A. Tejani, J. Totz, Z. Wang, and W. Shi. 2017. Photo-Realistic Single Image Super-Resolution Using a Generative Adversarial Network. In *2017 IEEE Conference on Computer Vision and Pattern Recognition*.
- [14] J. Lei Ba, J. R. Kiros, and G. E. Hinton. 2016. Layer Normalization. *ArXiv preprint arXiv: 1607.06450* (2016).
- [15] M.-Y. Liu, T. Breuel, and J. Kautz. 2017. Unsupervised Image-to-Image Translation Networks. In *Advances in Neural Information Processing Systems 30*.
- [16] M.-Y. Liu and O. Tuzel. 2016. Coupled Generative Adversarial Networks. In *Advances in Neural Information Processing Systems 29*.
- [17] Z. Liu, P. Luo, X. Wang, and X. Tang. 2015. Deep Learning Face Attributes in the Wild. In *Proceedings of International Conference on Computer Vision*.
- [18] Y. Lu, Y.-W. Tai, and C.-K. Tang. 2017. Attribute-Guided Face Generation Using Conditional CycleGAN. *ArXiv preprint arXiv: 1705.09966* (2017).
- [19] Z. Lu, T. Hu, L. Song, Zhaoxiang Zhang, and R. He. 2018. Conditional Expression Synthesis with Face Parsing Transformation. In *Proceedings of the 26th ACM International Conference on Multimedia*.
- [20] L. Ma, X. Jia, Q. Sun, B. Schiele, T. Tuytelaars, and L. Van Gool. 2017. Pose Guided Person Image Generation. In *Advances in Neural Information Processing Systems 30*.
- [21] X. Mao, Q. Li, H. Xie, R. Y. K. Lau, Z. Wang, and S. P. Smolley. 2016. Least Squares Generative Adversarial Networks. *ArXiv preprint arXiv: 1611.04076* (2016).
- [22] M. Mirza and S. Osindero. 2014. Conditional Generative Adversarial Nets. *ArXiv preprint arXiv: 1411.1784* (2014).
- [23] T. Miyato and M. Koyama. 2018. cGANs with Projection Discriminator. In *International Conference on Learning Representations*.
- [24] G. Perarnau, J. van de Weijer, B. Raducanu, and J. M. Álvarez. 2016. Invertible Conditional GANs for image editing. *ArXiv preprint arXiv: 1611.06355* (2016).
- [25] A. Radford, L. Metz, and S. Chintala. 2015. Unsupervised Representation Learning with Deep Convolutional Generative Adversarial Networks. *ArXiv preprint arXiv: 1511.06434* (2015).
- [26] L. Song, Z. Lu, R. He, Z. Sun, and T. Tan. 2018. Geometry Guided Adversarial Facial Expression Synthesis. In *Proceedings of the 26th ACM International Conference on Multimedia*.
- [27] T.-C. Wang, M.-Y. Liu, J.-Y. Zhu, A. Tao, J. Kautz, and Bryan Catanzaro. 2018. High-Resolution Image Synthesis and Semantic Manipulation With Conditional GANs. In *The IEEE Conference on Computer Vision and Pattern Recognition*.
- [28] T. Xu, P. Zhang, Q. Huang, H. Zhang, Z. Gan, X. Huang, and X. He. 2018. AttnGAN: Fine-Grained Text to Image Generation With Attentional Generative Adversarial Networks. In *The IEEE Conference on Computer Vision and Pattern Recognition*.
- [29] X. Yang, D. Xie, and X. Wang. 2018. Crossing-Domain Generative Adversarial Networks for Unsupervised Multi-Domain Image-to-Image Translation. In *Proceedings of the 26th ACM International Conference on Multimedia (MM '18)*. ACM, New York, NY, USA, 374–382.
- [30] Z. Yi, H. Zhang, P. Tan, and M. Gong. 2017. DualGAN: Unsupervised Dual Learning for Image-to-Image Translation. *ArXiv preprint arXiv: 1704.02510* (2017).
- [31] H. Zhang, T. Xu, H. Li, S. Zhang, X. Wang, X. Huang, and D. Metaxas. 2017. StackGAN: Text to Photo-Realistic Image Synthesis with Stacked Generative Adversarial Networks. In *2017 IEEE International Conference on Computer Visions*.
- [32] R. Zhang, S. Tang, Y. Li, J. Guo, Y. Zhang, J. Li, and S. Yan. 2018. Style Separation and Synthesis via Generative Adversarial Networks. In *Proceedings of the 26th ACM International Conference on Multimedia*.
- [33] J. Zhu, T. Park, P. Isola, and A. A. Efros. 2017. Unpaired Image-to-Image Translation Using Cycle-Consistent Adversarial Networks. In *2017 IEEE International Conference on Computer Vision*.
- [34] S. Zhu, S. Fidler, R. Urtasun, D. Lin, and C. L. Chen. 2017. Be Your Own Prada: Fashion Synthesis with Structural Coherence. In *Proceedings of the IEEE Conference on International Conference on Computer Vision*.